applied sciences

MDPI

Article

Experimental Study of Interference Effects of a High-Rise Building on the Snow Load on a Low-Rise Building with a Flat Roof

Qingwen Zhang [1,2], Yu Zhang [1,2], Ziang Yin [1,2], Guolong Zhang [1,2,*], Huamei Mo [1,2,*] and Feng Fan [1,2]

[1] Key Laboratory of Structures Dynamic Behavior and Control of the Ministry of Education, Harbin Institute of Technology, Harbin 150090, China; zhangqw@hit.edu.cn (Q.Z.); zhangyuhit@hit.edu.cn (Y.Z.); 17B933055@stu.hit.edu.cn (Z.Y.); fanf@hit.edu.cn (F.F.)

[2] Key Laboratory of Smart Prevention and Mitigation of Civil Engineering Disasters of the Ministry of Industry and Information Technology, Harbin Institute of Technology, Harbin 150090, China

* Correspondence: zhanggl315@hit.edu.cn (G.Z.); mohuamei@hit.edu.cn (H.M.)

Abstract: To explore the interference effects of a high-rise building on the snow load on a low-rise building with a flat roof, a series of wind tunnel tests were carried out with fine silica sand as a substitute for snow particles. The effects of the height of the interfering building and the distance between buildings on the snow distribution of the target building under three different wind directions were studied. The snow depth on the target building roof and the mass of particles blown off from the target building were measured during the wind tunnel tests, and the results showed that the snow distribution of the target building roof tends to be uniform when the interfering building is located upstream of the target building due to the shelter effect. When the interfering building is on the side of the target building, the snow distribution of the target building tends to be more uneven, because the interfering building increases the friction velocity on the target building roof near the interfering building. However, when the interfering building is located downstream of the target building, there will be an amplification effect of snow accumulation, and the snow distribution on the target building roof is nearly the same as that of the isolated condition. Under each wind direction, the interference effect of the snow load increases with the increase of the building height and the decrease of the building spacing. Therefore, the influence of the surrounding buildings on the snow distribution of the building roof cannot be ignored and should be considered in the structure design.

Keywords: snow load; interference effects; wind tunnel tests; snow distribution

Citation: Zhang, Q.; Zhang, Y.; Yin, Z.; Zhang, G.; Mo, H.; Fan, F. Experimental Study of Interference Effects of a High-Rise Building on the Snow Load on a Low-Rise Building with a Flat Roof. *Appl. Sci.* **2021**, *11*, 11163. https://doi.org/10.3390/app112311163

Academic Editor: Joan Formosa Mitjans

Received: 25 October 2021
Accepted: 20 November 2021
Published: 24 November 2021

1. Introduction

Structure collapses caused by blizzards are a common phenomenon, which has caused many casualties and huge economic losses. The uneven distribution of snow load caused by snowdrift is one of the main reasons for structures being damaged by heavy snow. The snow distribution on the roof of a building is mainly influenced by the wind field around the building. In urban cities, there are always buildings adjacent to a certain building, which will seriously affect the wind field in the vicinity, and it will affect the friction velocity on the building. This will result in a completely different form of snow distribution on the building when compared with the isolated condition. Figure 1 shows a 3D model of a typical case of snow distributions on a group of buildings in Harbin, China, which was built by pictures taken by drones. Thus, it is necessary to carry out relevant studies on the snow load interference effect.

Experimental research is the most effective tool used to investigate snowdrift. However, the mechanism of snowdrift is complicated, and it is difficult to choose similar criteria to conduct wind tunnel tests. Plenty of significant works investigating snowdrift have been done by scholars through wind tunnel tests. Wind tunnel tests of a road snow fence were carried out by Iversen (1981) [1] using glass spheres as a substitute for snow particles,

and the results of the wind tunnel tests were compared with the observation results. Anno (1984) [2] conducted wind tunnel tests of different sizes of snow fences and pointed out that the limit of the Froude number can be relaxed. This study also proposed a time similarity criterion based on snow flux. Delpech et al. (1998) [3] proposed a similarity criterion focusing on the similarity of the final drift snow volume and simulated the snow distribution around the Concordia Scientific Research Station in Antarctica by spraying artificial snow particles with a snow gun in the Jules Verne climate wind tunnel in France. Beyers and Harms (2003) [4] measured the snow distribution around the scaled model of the SANAE IV research station in Antarctica, especially in the wake region, and the influence of similarity criteria was discussed. Okaze et al. (2012) [5] conducted snow blowing tests on flat snow surfaces in a wind tunnel, and pointed out that the influence of snow particles on the wind field cannot be ignored in the saltation layer. Tominaga et al. (2013) [6] measured the velocity of saltating snow particles by using PIV measurements.

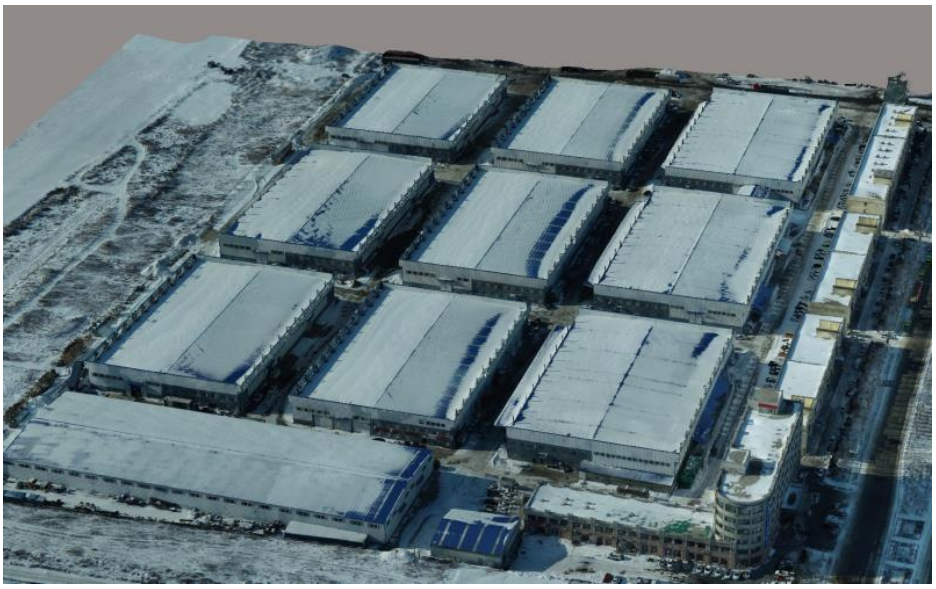

Figure 1. Three-dimensional model of snow distributions on a group of buildings in Harbin, China.

Although the studies mentioned above provided a deep investigation of the test particles and similarity criteria, they mainly focused on snowdrifts on the ground. Currently, there are fewer experimental studies of snowdrift on building roofs. Isyumov and Mikitiuk (1990) [7] used bran as substitute particles to carry out wind tunnel tests with different wind velocities and terrain roughness for stepped flat roofs. It was pointed out that the main factor affecting the snow distribution in rough terrain is the surrounding environment rather than particles' saltation. Tsuchiya et al. (2002) [8] measured the wind velocity on the surface of a stepped roof through a wind tunnel test, then analyzed the relationship between the wind velocity and the snow depth obtained by field observation. A negative correlation between the snow depth and the acceleration of the wind velocity near the roof was detected, which was consistent with the result derived by Scott et al. (1996) [9]. O'Rourke et al. (2004) [10] adopted crushed walnut to conduct water flume tests on a double pitched roof and a stepped flat roof, pointing out the feasibility of a water flume test. Zhou et al. (2014) [11] conducted wind tunnel tests with three kinds of particles, and the results were compared with field observations conducted by Tsuchiya et al. (2002) [8]. The best results can be obtained when silica sand is used as the substitute particles, thus fine silica sand was also used as substitute particles in this paper, although some similar criteria were not satisfied due to the limitation of the particle properties. Zhou et al. (2016) [12] conducted a wind tunnel test of snowdrifts on a flat roof using the same method as the reference [11]. The wind tunnel test was combined with the CFD (computational fluid

dynamics) numerical simulation by considering the repose angle of snow particles. Both results show favorable agreement.

It should be pointed out that scant studies investigating the snow load interference effect have been done. Flaga, A. and Flaga, Ł (2019) [13] performed wind tunnel tests of the snow load distribution on three different large-sized stadium roofs by using powdered polystyrene foam as artificial snow, and the interference effect between the investigated object and its surroundings was pointed out. Beyers and Waechter (2008) [14] simulated the snowdrifts around three adjacent elevated buildings and compared the results with field observations. Overall, the prediction results corresponded well with the actual snowdrift pattern. Thiis and Ferreira (2015) [15] investigated the snow deposition around three different geometrical configurations of pillars using the CFD method. Based on the results, an arrangement was proposed for the design of windbreaks. Okaze et al. (2016) [16] explored the performance of the CFD method in predicting the snowdrift in and around a building array. The simulated snow distribution pattern showed good agreement with the field measurement conducted by Tsutsumi et al. (2012) [17]. The influence of surrounding buildings is also considered by the exposure coefficient in the ISO 4355 code (2013) [18], but the provision is considered to be nominal.

Previous studies have focused on the wind interference effect, and the research methods of related studies may contain an important reference for the study of the snow load interference effect. Case and Isyumov (1998) [19] studied the influence of different wind field exposure conditions on the wind load of a double slope roof with a slope of 4:12 through a wind tunnel test. It was pointed out that when a simple building is embedded in a series of similar buildings, the wind load will be reduced due to the interference. Chang and Meroney (2003) [20] investigated the influence of surrounding buildings on the wind load of low flat-roofed buildings and pointed out the shelter effect of surrounding buildings. Kim et al. (2012) [21] conducted similar but more detailed research on the interference effect of buildings on low flat-roofed buildings. Pindado (2011) [22] studied the interference effect of a high-rise building on a low flat-roofed building and obtained a conclusion different from that derived from studies on the interference of a series of buildings. Chen et al. (2018) [23] conducted a huge number of wind tunnel tests to discuss the wind interference effect of a high-rise interfering building on a low-rise target building with a flat roof in more detail.

As mentioned above, the previous studies have mainly focused on the snowdrift on an isolated building or snowdrifts on the ground around a group of buildings. Scant research has investigated snowdrifts on the roofs of a building array and the interference effect between them. Actually, buildings are located near interfering buildings in urban cities. The structures may face more threats of snow disaster if we ignore the interference effects on snow loads. Hence, a series of wind tunnel tests were carried out in this paper, to explore the interference effects of a high-rise building on the snow load on a low-rise building with a flat roof. Snow distributions on the target building were measured, based on which the effects of the height of the interfering building and the distance between buildings on the snow distribution of the target building under three wind directions were discussed.

2. Materials and Methods

2.1. Similarity Criteria

Snow drifting can be explained as a particle transport process. Depending on whether the friction velocity reaches a threshold value, three transport sub-processes can be observed, namely, creep, saltation, and suspension. Creep is a sub-process in which snow particles move by rolling or creeping near the snow surface; saltation is a sub-process in which snow particles move with jumping and colliding with the snow surface; and at a higher wind velocity, particles are transported upwards by turbulence and transported far downwind. Among the sub-processes, saltation is identified as the major particle transport sub-process.

To make the wind tunnel tests quantitatively reflect the prototype, the similarity criteria need to be met. However, due to the contradiction of some similarity criteria and the limitation of the particle properties, some similarity criteria must be relaxed. The typical similarity criteria used in this paper are briefly listed as follows:

2.1.1. Modeling of the Wind Field

Kind (1976) [24] pointed out that it is necessary to guarantee the lower limit of the Reynolds number $u^{*3}/2gv > 30$ to model the fully turbulent saltation flow. If the saltation sub-process occurs ($u^* > u_t^*$), the fully turbulent flows will be satisfied by Equation (1). This similarity number has been widely adopted by scholars:

$$\frac{u_t^{*3}}{2gv} > 30, \tag{1}$$

where u^* represents the friction velocity, u_t^* is the threshold friction velocity, g is the gravitational acceleration, and v is the turbulent viscosity.

Iverson (1981) [1] believed that the similarity of the aerodynamic roughness height caused by saltation particles should be met, shown as Equation (2). However, Zhou et al. (2016) [12] anticipated that for a building that has significant flow separation occurring at the eave, the aerodynamic roughness height is no longer mainly caused by saltation particles; hence, the similarity requirement of Equation (2) could be relaxed:

$$\left(\frac{\rho u^{*2}}{\rho_s H g}\right)_m = \left(\frac{\rho u^{*2}}{\rho_s H g}\right)_p, \tag{2}$$

where ρ is the density of air, ρ_s is the density of particles, and H is the eave height. The subscripts "m" and "p" represent the model and prototype, respectively.

2.1.2. Modeling of the Ejection Process

To guarantee the dynamic similarity correctly, Iverson (1981) [1] proposed a densimetric Froude number of particles (the ratio between the inertia force and gravity force of particles), as shown in Equation (3). In order to simulate the starting condition of saltation, the ratio of the wind velocity and the threshold friction velocity should be satisfied [24], as shown in Equation (4). Furthermore, Kind (1986) [25] suggested that heavy particles should be used to ensure good similarity of the densimetric Froude number, and hence the requirement of Equation (5) should be met:

$$\left(\frac{\rho}{\rho_s - \rho}\frac{u_t^{*2}}{g d_s}\right)_m = \left(\frac{\rho}{\rho_s - \rho}\frac{u_t^{*2}}{g d_s}\right)_p, \tag{3}$$

$$\left(\frac{U(H)}{u_t^*}\right)_m = \left(\frac{U(H)}{u_t^*}\right)_p, \tag{4}$$

$$\rho_s/\rho > 600, \tag{5}$$

where d_s is the diameter of particles and $U(H)$ is the wind velocity at the eave height.

2.1.3. Modeling of the Particle Trajectory

To ensure the similarity of the trajectory of saltating particles between the wind tunnel tests and the prototype, Kind (1986) [25] believed that Equation (6) must be met. Furthermore, it is necessary to maintain a similar ratio of the falling velocity of particles and the horizontal velocity as shown in Equation (7):

$$\left(\frac{\rho_s}{\rho_s - \rho}\frac{U(H)^2}{gH}\right)_m = \left(\frac{\rho_s}{\rho_s - \rho}\frac{U(H)^2}{gH}\right)_p, \tag{6}$$

$$\left(\frac{W_f}{U(H)}\right)_{\mathrm{m}} = \left(\frac{W_f}{U(H)}\right)_{\mathrm{p}}, \tag{7}$$

where W_f is the falling velocity of particles.

2.1.4. Similar Deposit Pattern

The angle of repose refers to the angle formed between the surface of the accumulation and the horizontal plane when particles are accumulated into a cone. Therefore, a similar angle of repose should be satisfied to reproduce similar snow deposit patterns [25], as shown in Equation (8). However, due to the different properties of snow particles and artificial particles, Equation (8) cannot be met favorably:

$$(\theta)_{\mathrm{m}} = (\theta)_{\mathrm{p}}, \tag{8}$$

where θ is the response angle of particles.

2.1.5. Time Similarity

The evaluation of the equivalent model snowfall duration with respect to the prototype snowfall duration is one of the main difficulties in the experimental snow drifting modellings. Here, a time similarity number [24], which focuses on the similarity of the accumulation volume of snow during a certain duration, is adopted, as shown in Equation (9):

$$\left(\frac{\rho}{\rho_{\mathrm{s}}}\frac{U(H)}{H}T\right)_{\mathrm{m}} = \left(\frac{\rho}{\rho_{\mathrm{s}}}\frac{U(H)}{H}T\right)_{\mathrm{p}}, \tag{9}$$

where T represents the duration of the snowstorm.

2.2. Regime of the Wind Tunnel Test

Wind tunnel tests were conducted with fine silica sand as the substitute for snow particles in this paper. The physical properties of the snow particles and fine silica are shown in Table 1.

Table 1. Physical properties of snow particles and fine silica.

Parameters	Snow Particles	Fine Silica
Density ρ_{s} (kg/m^3)	250	2650
Diameter d_{s} (mm)	0.15	0.2
Settling velocity W_f (m/s)	0.2~1.0 m/s	0.6
Threshold friction velocity u^*_{t} (m/s)	0.2	0.26
Angle of repose θ (°)	50°	34°

To study the interference effects of a high-rise building on the snow load on a low-rise building with a flat roof, two models were adopted: one is the interfering building and the other is the target building. The model scale ratio is 1:50, and the size of the target building model is 15 cm × 15 cm × 8 cm. The influences of the height of the interfering building and the distance between buildings on the snow distribution of the target building under three different wind directions are discussed. A schematic diagram of the wind tunnel tests is shown in Figure 2. The height of the target building is defined as $H0$, the height of the interfering building is defined as H, and the distance between the target building and the interfering building is defined as D. The interfering building height is set to be 1, 2, 3, or 4 times that of the target building, and the distance between buildings is set to be 1, 2, or 3 times the height of the target building. The length of the wind tunnel is 6m, the section size is 1.2m×1m, and the blocking rate of the wind tunnel is less than 5%.

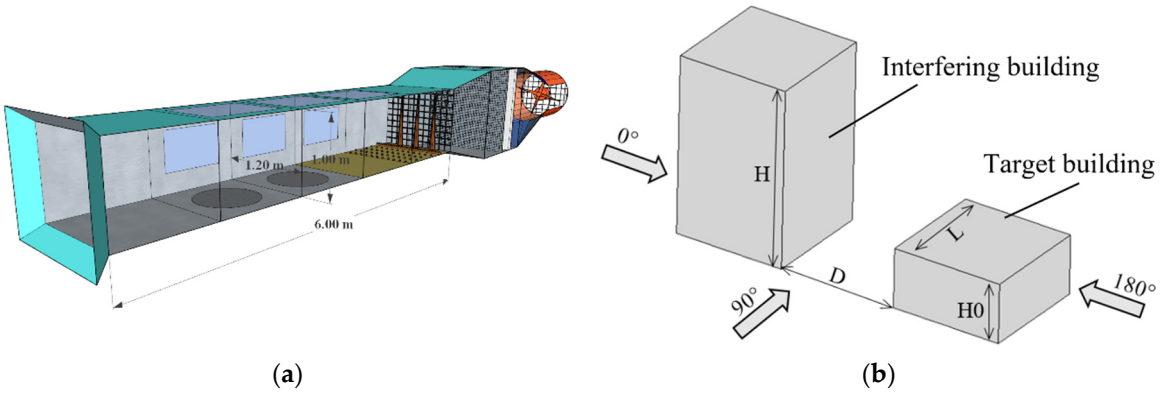

(**a**) (**b**)

Figure 2. Schematic diagram of the wind tunnel tests: (**a**) wind tunnel diagram; (**b**) building configuration.

For comparison, a test on the isolated target building was also carried out; hence, there are $3 \times 4 \times 3 + 1 = 37$ wind tunnel tests in total. First, 9-mm-thick fine silica sand particles are laid on the roof of the target building model before the wind tunnel tests, corresponding to a 0.45-m-thick snow depth for the prototype. If the bulk density of snow is 150 kg/m^3, the snow depth of 0.45 m corresponds to the basic snow pressure in Harbin, China. The wind velocity at the eave height of the low-rise building model is set as 7 m/s, and the profiles of the mean wind velocity and turbulent intensity are shown in Figure 3. The reference height H_{ref} is 0.08 m, and the reference wind velocity U_{ref} is 7 m/s. The average wind velocity profile follows the logarithmic rate distribution. The friction velocity is 0.21 m/s, and the roughness height is 0.000205 m.

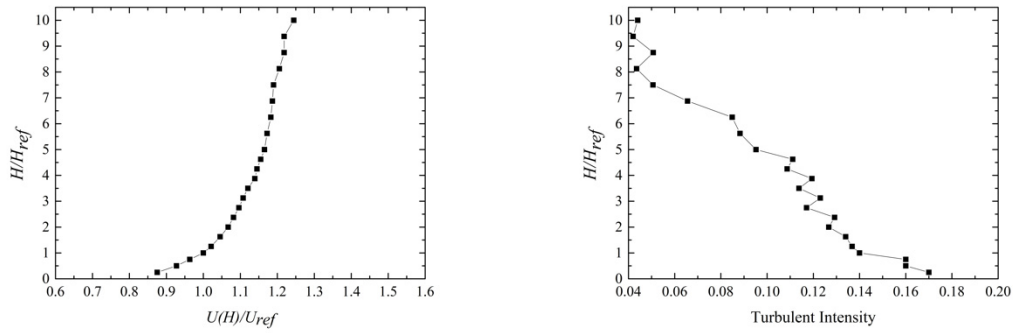

(**a**) (**b**)

Figure 3. Inflow wind field of the experiment: (**a**) normalized mean wind velocity; (**b**) turbulent intensity.

The parameters of the wind tunnel tests and prototypes are shown in Table 2. The eave height of the target building of the prototype is 4 m, and the time duration of the prototype is 29.1 min. The similarity criteria are listed in Table 3. Due to the limitation of the particle properties, not all similarity criteria are matched. The Reynolds number of the aerodynamic roughness height of the tests $u_{\mathrm{t}}^{*3}/2gv > 30$ maintains the fully developed turbulent flow. The densimetric Froude numbers of the tests are different from that of the prototype. However, Anno (1984) [2], Zhou et al. (2014) [11], and Zhou et al. (2016) [12] conducted contrast tests of different particles and pointed out that the Froude number has minimal influence on the final pattern of the redistribution of snow. Thus, the similarity parameters $(\rho/\rho_{\mathrm{s}} - \rho)\left(u_{\mathrm{t}}^{*2}/gd_{\mathrm{s}}\right)$ and $(\rho_{\mathrm{s}}/\rho_{\mathrm{s}} - \rho)\left(U(H)^2/gH\right)$ could be relaxed. The heavy particle requirement similarity parameter $\rho_{\mathrm{s}}/\rho > 600$ is satisfied. The settling velocity of snow particles may range from 0.2~1.0 m/s, thus the similarity criteria $W_f/U(H)$ are satisfied. As mentioned before, the main purpose of this paper was to investigate snow load interference effects rather than reproduce a specific prototype, thus it is acceptable to relax some of the similarity criteria.

Table 2. Parameters of the wind tunnel tests and prototypes.

Description	Prototype	Wind Tunnel Test
Eave height of the target building (m)	4	0.08
Wind velocity at eave height (m/s)	5.4	7
Initial snow depth (cm)	45	0.9
Time duration (min)	29.1	5

Table 3. Similarity parameters.

Similarity Parameters	Prototype	Wind Tunnel Test
$\frac{u_t^{*3}}{2gv} > 30$		61.8
$\frac{\rho}{\rho_s-\rho}\frac{u_t^{*2}}{gd_s}$	0.134	0.015
$\frac{U(H)}{u_t^*}$	27	27
$\rho_s/\rho > 600$		2272.7
$\frac{\rho_s}{\rho_s-\rho}\frac{U(H)^2}{gH}$	0.8	62.5
$\frac{W_f}{U(H)}$	0.037~0.185	0.086
$\frac{\rho}{\rho_s}\frac{U(H)}{H}T$	2.3	2.3

3. Results and Discussion

Typical photos of the tests are shown in Figure 4. The working conditions are represented by the case number, such as "$D/H0$"–"$H/H0$"–"WD (Wind Direction)". Here, the case number of "isolated" represents the wind tunnel test of the target building without an interfering building.

Due to the limitation of the measuring equipment, only the snow depth of the central line along the wind direction on the target building was measured and normalized by the initial snow depth, and the results are shown in Figures 5–7. The $h0$ and h are the snow depths on the low-rise building roof before and after wind tunnel tests, respectively; "x" is the distance between the measured points and the windward eave.

According to Figure 4, the snow layer on the roof of the target building is two-dimensional for cases of wind directions of 0 and 180 degrees for the interfering building positioned upstream and downstream of the target building. In these conditions, the snow depth of the central line can represent the whole snow distribution on the target building. However, the snow layer on the target building for the 90-degree cases is highly three-dimensional for the buildings placed side by side. To describe the snow distribution of all conditions, the mass of particles blown off from the target building was also recorded and normalized by $m0$, which is the recorded mass of particles blown off from the target building under the isolated working condition, as shown in Figures 4–7. The snow depth of the central line combined with the mass of particles blown off from the target building and the photos of the experiments can reflect the overall situation of the experiments.

Figure 5 shows the results of cases for the wind direction of 0°, and the interfering building positioned upstream of the target building. The wind velocity of the target building at the eave height is decreased, and the snow in the front of the target building roof ($x/L < 0.4$) is significantly accumulated when compared with the case isolated due to the shelter effect of the interfering building. According to Figure 5, when $H/H0 = 1$, the wake flow of the interfering building leads to an increase of the friction velocity on the roof of the target building, where $x/L > 0.4$, resulting in a lower snow depth than that of the isolated condition. When $H/H0 > 1$, the snow depth on the target building is larger than that of the case isolated due to the shelter effect of the interfering building. The peak values of the normalized snow depth on the target building are larger than that of the isolated case. With the increase of the height of the interfering building (H), the snow distribution tends to be uniform, and more areas on the target roof are affected by the interfering building, and the shelter effect becomes powerful. With the increase of the

building spacing, the shielding area of the interfering building cannot cover the target building, thus the normalized snow depth becomes more similar to that of the isolated condition. The building spacing and the height difference between the two buildings seem to be the main influencing factors of the shelter effects.

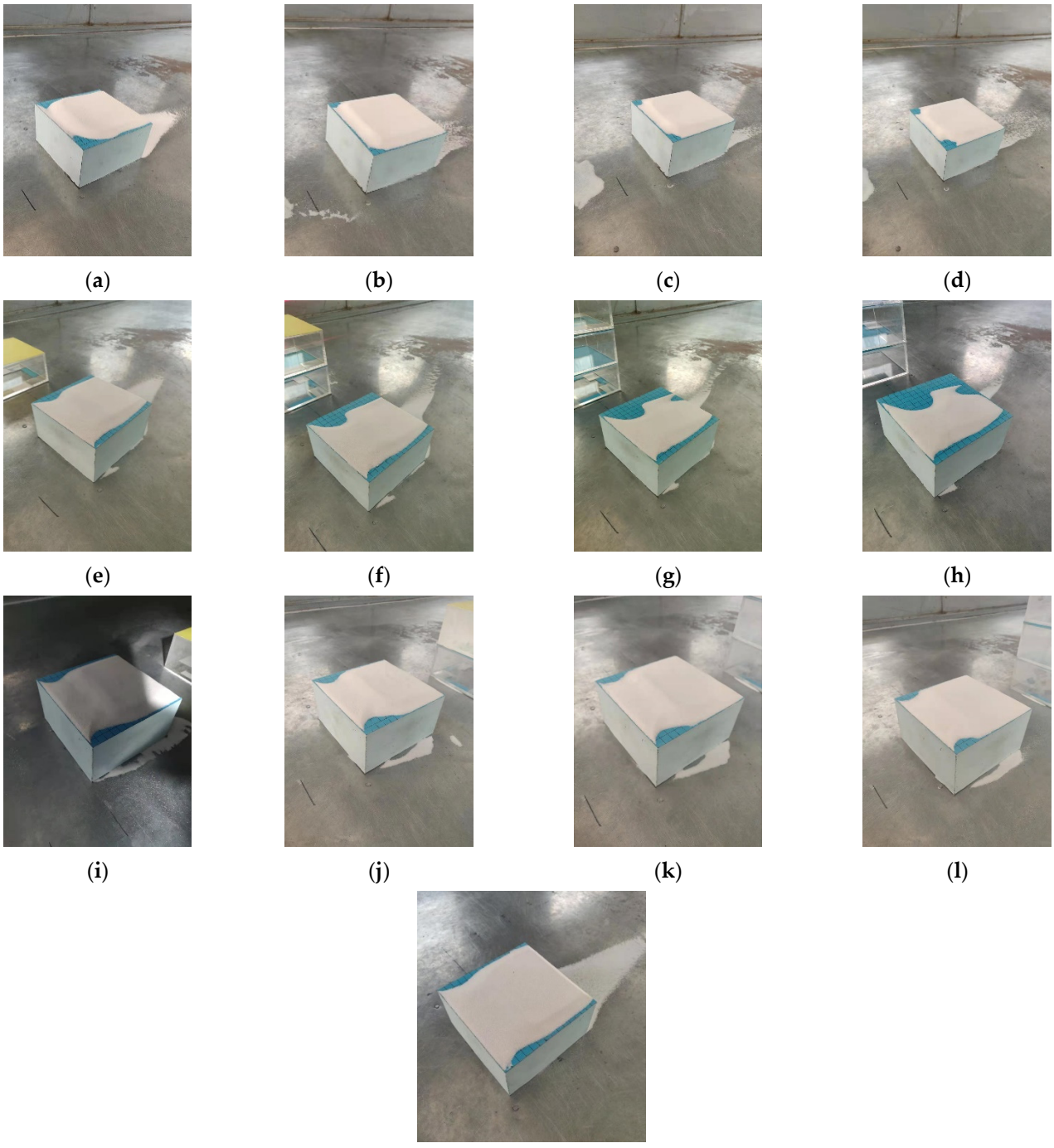

Figure 4. Photos of typical cases: (**a**) Case: $D/H0$ = 2—$H/H0$ = 1—*WD* 0°; (**b**) Case: $D/H0$ = 2—$H/H0$ = 2—*WD* 0°; (**c**) Case: $D/H0$ = 2—$H/H0$ = 3—*WD* 0°; (**d**) Case: $D/H0$ = 2—$H/H0$ = 4—*WD* 0°; (**e**) Case: $D/H0$ = 2—$H/H0$ = 1—*WD* 90°; (**f**) Case: $D/H0$ = 2—$H/H0$ = 2—*WD* 90°; (**g**) Case: $D/H0$ = 2—$H/H0$ = 3—*WD* 90°; (**h**) Case: $D/H0$ = 2—$H/H0$ = 4—*WD* 90°; (**i**) Case: $D/H0$ = 2—$H/H0$ = 1—*WD* 180°; (**j**) Case: $D/H0$ = 2—$H/H0$ = 2—*WD* 180°; (**k**) Case: $D/H0$ = 2—$H/H0$ = 3—*WD* 180°; (**l**) Case: $D/H0$ = 2—$H/H0$ = 4—*WD* 180°; (**m**) Case isolated.

As shown in Figure 5d, the mass of particles blown off from the target building is close to $m0$ when $H/H0 = 1$ and more particles are blown off the target building roof when compared with the isolated condition with the increase of the height of the interfering building and the decrease of the building spacing. The mass of particles blown off from the target building in case $D/H0 = 1$—$H/H0 = 2$—WD 0° is the least amongst all wind tunnel tests, which is around 33% of $m0$. An interesting phenomenon is observed that there are two erosion areas on both sides of the target building, and the eroded area decreases first and then increases instead of decreasing all the time with the increase of the height of the interfering building. Generally speaking, the snow distribution on the roof of the target building tends to be more uniform when the interfering building is positioned upstream of the target building.

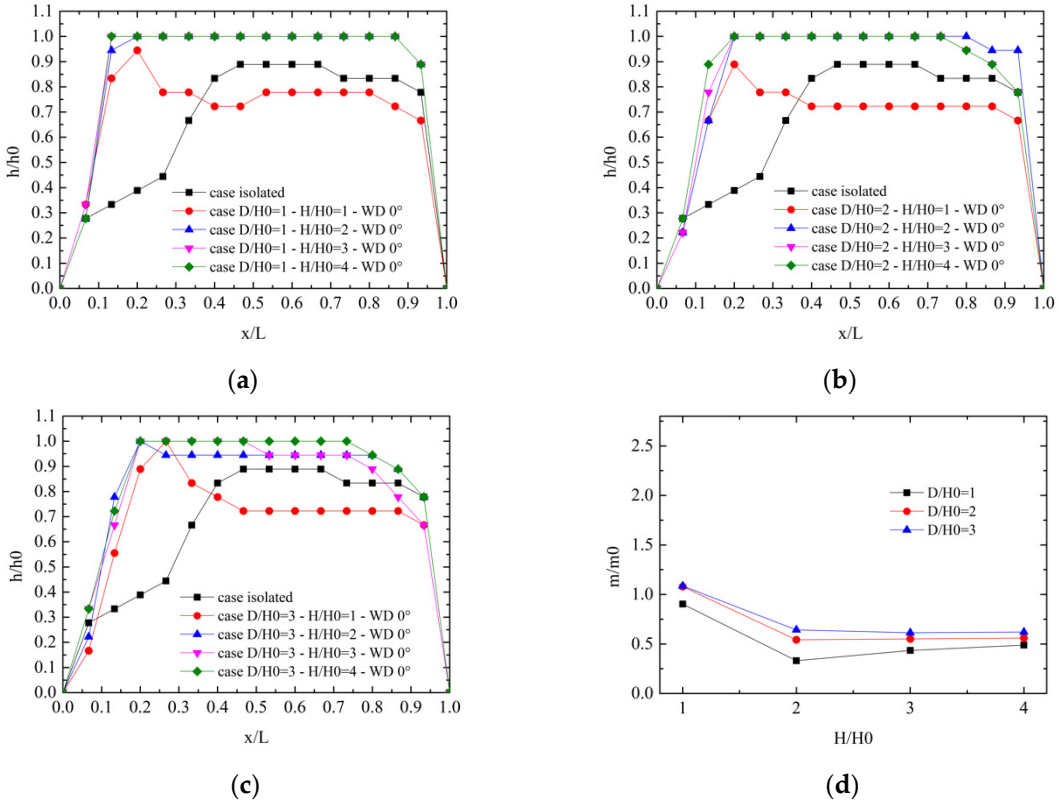

Figure 5. Experiment results of cases under the 0° wind direction: (**a**) building spacing: $D/H0 = 1$; (**b**) building spacing: $D/H0 = 2$; (**c**) building spacing: $D/H0 = 3$; (**d**) normalized mass of particles blown off the target building.

It can be seen from Figure 6 that when the wind direction is 90°, the interfering building is positioned at the side of the target building; the friction velocity on the target building significantly increases due to the interference. It results in a more eroded area on the target building, and the snow distribution on the target building roof tends to be more uneven. The part of the target building roof near the interfering building is seriously eroded, and particles are blown to the center of the target building and then accumulated, leading to a larger snow depth at the position where x/L is around 0.5 when compared with the isolated case, such as case $D/H0 = 1$—$H/H0 = 1$—WD 90° and case $D/H0 = 2$—$H/H0 = 1$—WD 90°. However, the part of the target building away from the interfering building is not affected. Thus, the snow distribution of the crosswind direction is seriously uneven; hence, the snow layer on the target building for the 90-degree cases is highly three-dimensional.

With the increase of the height of the interfering building (H), the interference effect becomes more powerful, and according to Figure 6d, more particles are blown off the target building roof. The mass of particles blown off from the target building in case $D/H0 =$

1—$H/H0$ = 4—*WD* 90° is the heaviest amongst all the wind tunnel tests, which is 2.67 times that of the case isolated. In this case, the normalized snow depth of the central line shows two peak values, and both the peak values are lower than 0.4. With the increase of the building spacing, the disturbance of the interfering building is weakened, fewer particles are blown off the target building roof, the snow distribution on the target building roof becomes more similar to that of the isolated case, and the form of the normalized snow depth changes from a bimodal distribution to a single peak distribution, as shown in Figure 6.

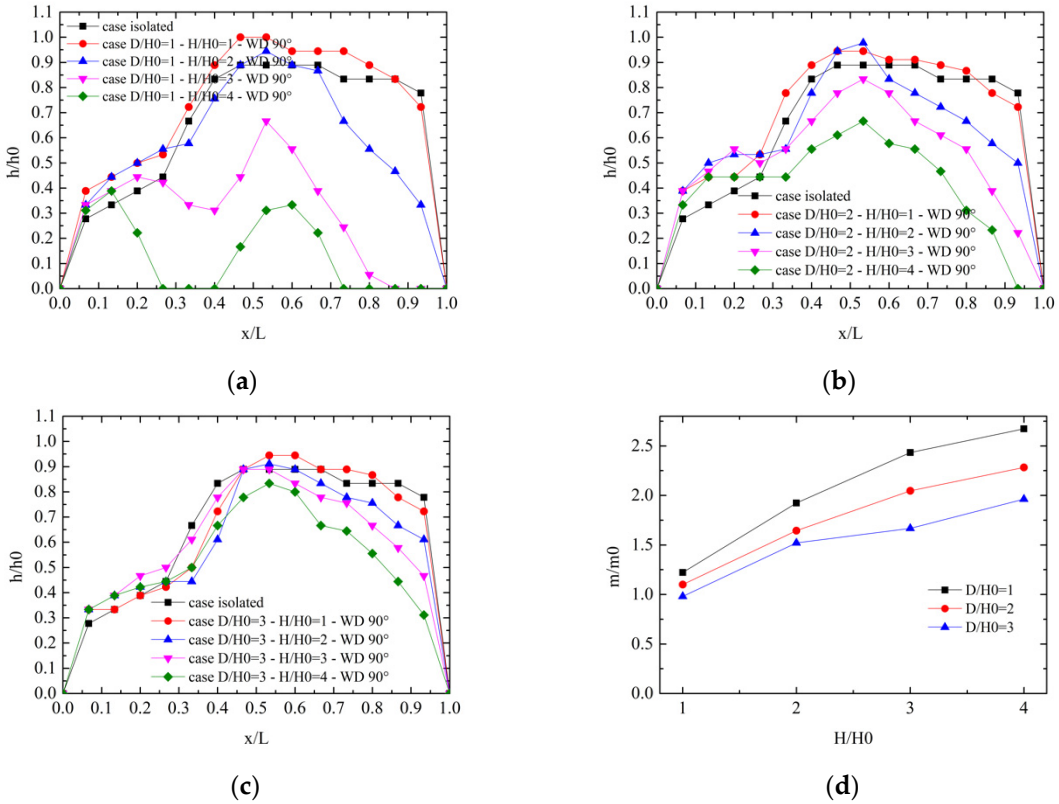

Figure 6. Normalized snow depth of the central line on the target building under the 90° wind direction: (**a**) building spacing: *H*0; (**b**) building spacing: 2*H*0; (**c**) building spacing: 3*H*0; (**d**) normalized mass of particles blown off the target building.

It can be seen from Figure 7 that when the wind direction is 180°, the interfering building is positioned downstream of the target building, and the flow separation form of the target building is unchanged; hence, the form of the snow distribution on the target building is nearly the same as the isolated case. However, the wind velocity of the target building is somewhat lower than the isolated condition because the wind is blocked by the interfering building; hence, the normalized snow depths are slightly amplified compared to the isolated case. When $D/H0 \geq 2$, the normalized snow depth is even bigger than 1 in the vicinity of the position where $x/L = 0.4$.

The amplification effect occurs if the interfering building is positioned downstream of the target building, and the amplification effect increases with the increase of the height of the interfering building and the decrease of the distance between the interfering building and the target building.

As shown in Figure 7d, when the wind direction is 180°, the amount of snow particles blown off the target building changes less with the increase of the height of the interfering building when compared with the cases under the other two wind directions. The snow distribution on the roof of the target building tends to be more uniform when the interfering building is positioned downstream of the target building.

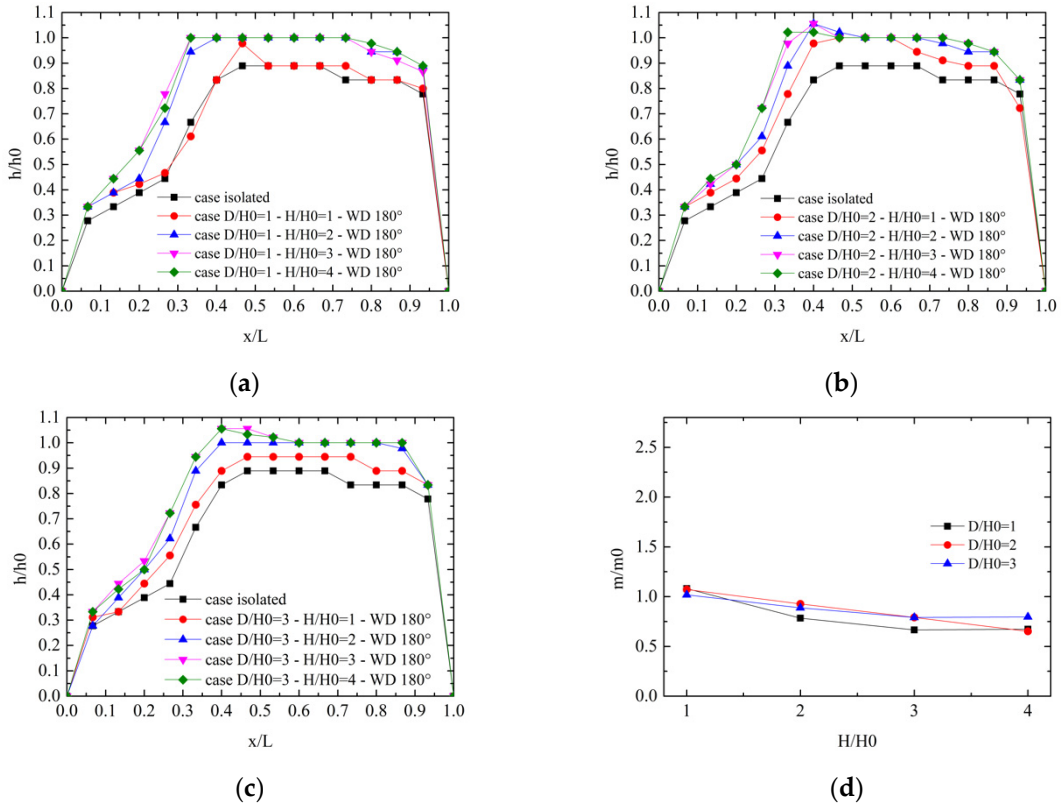

Figure 7. Normalized snow depth of the central line on the target building under the 180° wind direction: (**a**) building spacing: *H*0; (**b**) building spacing: 2*H*0; (**c**) building spacing: 3*H*0; (**d**) normalized mass of particles blown off the target building.

4. Conclusions

A series of wind tunnel tests were carried out with fine silica sand as a substitute for snow particles to explore the interference effects of a high-rise building on the snow load on a low-rise building with a flat roof. The effects of the interfering building height and the distance between buildings on the snow distribution of the target building under three wind directions were discussed, and the following conclusions can be drawn.

1. When the wind direction is 0° and the interfering building is positioned upstream of the target building, due to the shelter effect of the interfering building, the wind velocity is much weakened compared with the isolated condition. As a result, the snow distribution tends to be more uniform.
2. When the wind direction is 90° and the interfering building is on the side of the target building, a more eroded area appears on the target building roof due to the increasing friction velocity on the target building, and the snow distribution on the target building tends to be more uneven.
3. When the wind direction is 180° and the interfering building is positioned downstream of the target building, the target building is located at the back flow area caused by the interfering building, and there are amplification effects of snow accumulation on the target building. The forms of the snow distribution on the target building are nearly the same as that of the isolated condition.
4. Under each wind direction, the interference effect of the snow load increases with the increase of the building height and the decrease of the building spacing.

The influence of the surrounding buildings on the snow distribution of the building roof cannot be ignored and should be considered in the structure design. It may be helpful to mitigate the negative effects of interference if the building under construction is close to

the height of the surrounding buildings. More attention should be paid to the snow load interference effects in the future.

Author Contributions: Conceptualization, Q.Z. and F.F.; methodology, Z.Y.; software, H.M.; validation, Y.Z., Z.Y. and G.Z.; formal analysis, G.Z.; investigation, Z.Y.; resources, Q.Z.; data curation, F.F.; writing—original draft preparation, Z.Y.; writing—review and editing, G.Z.; visualization, Y.Z.; supervision, H.M.; project administration, F.F.; funding acquisition, Q.Z. and F.F. All authors have read and agreed to the published version of the manuscript.

Funding: This research was funded by the Funds for Creative Research Groups of National Natural Science Foundation of China (grant number 51921006), Chinese National Natural Science Foundation project (grant number 51978207, 51927813, 51808169), National Science Fund for Distinguished Young Scholars (grant number 51525802), and Heilongjiang Natural Science Foundation for Excellent Youth project (grant number YQ2021E030).

Acknowledgments: The authors are grateful to the members of the Space Structure Research Center at the Harbin Institute of Technology, for providing invaluable information and advice in this study.

Conflicts of Interest: The authors declare no conflict of interest. The funders had no role in the design of the study; in the collection, analyses, or interpretation of data; in the writing of the manuscript, or in the decision to publish the results.

References

1. Iversen, J.D. Comparison of wind-tunnel model and full-scale snow fence drifts. *J. Wind Eng. Ind. Aerodyn.* **1981**, *8*, 231–249. [CrossRef]
2. Anno, Y. Requirements for modeling of a snowdrift. *Cold Reg. Sci. Technol.* **1984**, *8*, 241–252. [CrossRef]
3. Delpech, P.; Palier, P.; Gandemer, J. Snowdrifting Simulation around Antarctic Buildings. *J. Wind Eng. Ind. Aerodyn.* **1998**, *74–76*, 567–576. [CrossRef]
4. Beyers, J.H.M.; Harms, T.M. Outdoors modelling of snowdrift at SANAE IV Research Station, Antarctica. *J. Wind Eng. Ind. Aerodyn.* **2003**, *91*, 551–569. [CrossRef]
5. Okaze, T.; Mochida, A.; Tominaga, Y. Wind tunnel investigation of drifting snow development in a boundary layer. *J. Wind Eng. Ind. Aerodyn.* **2012**, *104–106*, 532–539. [CrossRef]
6. Tominaga, Y.; Okaze, T.; Mochida, A. PIV measurements of saltating snow particle velocity in a boundary layer developed in a wind tunnel. *J. Vis.* **2013**, *16*, 95–98. [CrossRef]
7. Isyumov, N.; Mikitiuk, M. Wind tunnel model tests of snow drifting on a two-level flat roof. *J. Wind Eng. Ind. Aerodyn.* **1990**, *36*, 893–904. [CrossRef]
8. Tsuchiya, M.; Tomabechi, T.; Hongo, T. Wind effects on snowdrift on stepped flat roofs. *J. Wind Eng. Ind. Aerodyn.* **2002**, *90*, 1881–1892. [CrossRef]
9. Scott, L.; Gamble, S.; Will, W. Finite Area Element Snow Loading Prediction—Applications and Advancements. *J. Wind Eng. Ind. Aerodyn.* **1996**, *42*, 1537–1548.
10. O'Rourke, M.; DeGaetanob, A.; Tokarczyk, J.D. Snow drifting transport rates from water flume simulation. *J. Wind Eng. Ind. Aerodyn.* **2004**, *92*, 1245–1264. [CrossRef]
11. Zhou, X.; Hu, J.; Gu, M. Wind tunnel test of snow loads on a stepped flat roof using different granular material. *Nat. Hazards* **2014**, *74*, 1629–1648. [CrossRef]
12. Zhou, X.; Kang, L.; Gu, M. Numerical simulation and wind tunnel test for redistribution of snow on a flat roof. *J. Wind Eng. Ind. Aerodyn.* **2016**, *153*, 92–105. [CrossRef]
13. Flaga, A.; Flaga, Ł. Wind tunnel tests and analysis of snow load distribution on three different large size stadium roofs. *Cold Reg. Sci. Technol.* **2019**, *160*, 163–175. [CrossRef]
14. Beyers, M.; Waechter, B. Modeling transient snowdrift development around complex three-dimensional structures. *J. Wind Eng. Ind. Aerodyn.* **2008**, *96*, 1603–1615. [CrossRef]
15. Thiis, T.; Ferreira, A.D. Sheltering effect and snow deposition in arrays of vertical pillars. *Environ. Fluid Mech.* **2015**, *15*, 27–39. [CrossRef]
16. Okaze, T.; Kato, S.; Tominaga, Y. CFD prediction of snowdrift in a building array. In Proceedings of the 8th International Conference on Snow Engineering, Nantes, France, 14–17 June 2016; pp. 26–29.
17. Tsutsumi, T.; Chiba, T.; Tomabechi, T. Snowdrifts on and around buildings based on field measurement. In Proceedings of the 7th International Conference on Snow Engineering, Fukui, Japan, 6–8 June 2012; pp. 9–17.
18. ISO 4355. *Bases for Design of Structures Determination of Snow Loads on Roofs*, 3rd ed.; ISO: Geneva, Switzerland, 2013; pp. 4–5.
19. Case, P.C.; Isyumov, N. Wind loads on low buildings with 4:12 gable roofs in open country and suburban exposures. *J. Wind Eng. Ind. Aerodyn.* **1998**, *77–78*, 107–118. [CrossRef]

20. Chang, C.H.; Meroney, R.N. The effect of surroundings with different separation distances on surface pressures on low-rise buildings. *J. Wind Eng. Ind. Aerodyn.* **2003**, *91*, 1039–1050. [CrossRef]
21. Kim, Y.C.; Yoshida, A.; Tamura, Y. Characteristics of surface wind pressures on low-rise building located among large group of surrounding buildings. *Eng. Struct.* **2012**, *35*, 18–28. [CrossRef]
22. Pindado, S.; Meseguer, J.; Franchini, S. Influence of an upstream building on the wind-induced mean suction on the flat roof of a low-rise building. *J. Wind Eng. Ind. Aerodyn.* **2011**, *99*, 889–893. [CrossRef]
23. Chen, B.; Shang, L.; Qin, M. Wind interference effects of high-rise building on low-rise building with flat roof. *J. Wind Eng. Ind. Aerodyn.* **2018**, *183*, 88–113. [CrossRef]
24. Kind, R.J. A critical examination of the requirements for model simulation of wind-induced erosion/deposition phenomena such as snow drifting. *Atmos. Environ.* **1976**, *10*, 219–227. [CrossRef]
25. Kind, R.J. Snowdrifting: A review of modeling methods. *Cold Reg. Sci. Technol.* **1986**, *12*, 217–228. [CrossRef]